AIP Advances

Local mechanical and electrical behavior in CdTe thin film solar cells revealed by scanning probe microscopy

Cite as: AIP Advances **9**, 085108 (2019); https://doi.org/10.1063/1.5093906
Submitted: 25 February 2019 . Accepted: 01 August 2019 . Published Online: 13 August 2019

Melissa Mathews, Liping Guo, Xiao Han, Swapnil Saurav, Guozhong Xing, Lin Li, and Feng Yan

Local mechanical and electrical behavior in CdTe thin film solar cells revealed by scanning probe microscopy

Cite as: AIP Advances 9, 085108 (2019); doi: 10.1063/1.5093906
Submitted: 25 February 2019 • Accepted: 1 August 2019 •
Published Online: 13 August 2019

Melissa Mathews,[1] Liping Guo,[2] Xiao Han,[2] Swapnil Saurav,[2] Guozhong Xing,[3] Lin Li,[2] and Feng Yan[2,a)]

AFFILIATIONS

[1]Department of Chemical and Biological Engineering, The University of Alabama, Tuscaloosa, Alabama 35487, USA
[2]Department of Metallurgical and Materials Engineering, The University of Alabama, Tuscaloosa, Alabama 35487, USA
[3]United Microelect Corp. Ltd., 3 Pasir Ris Dr 12, Singapore, 519528, Singapore

[a)]**Corresponding author; email:** fyan@eng.ua.edu

ABSTRACT

The nanoscale electrical and mechanical properties in the CdTe thin films solar cells were investigated using the scanning probe microscopy. The comparative localized electrical and mechanical properties between as-grown and $CdCl_2$ treated CdTe thin films for the grain and grain boundaries were studied using the conductive atomic force microscopy (cAFM) and force modulation microscopy (FMM). An increased electrical behavior and decreased elastic stiffness in the $CdCl_2$ treated thin films were recorded to elucidate the impact from the grain growth of CdTe grains. On applying a simulated working electrical bias into the CdTe thin-film solar cells, the electric field across the CdTe film can increase the softness of CdTe thin film. The results imply the presence of a potential mechanical failure site in the CdTe grain boundary, which may lead to device degradation.

Thin film solar cells have a growing interest in the solar energy market because of their low-cost production processes and opportunity for flexible cell applications.[1–3] The power conversion efficiency (PCE) of thin film solar cells (e.g., CdTe, CuInGaSe, and Perovskites) have been improved to 22% via engineering the electronic and optical properties.[4–7] CdTe technology is the most successful commercial thin-film solar cell. For example, *First Solar* has manufactured more than 17 GW CdTe solar modules by 2018.[7] To understand the mechanisms of efficiency loss in the CdTe solar cells, the nanoscale charge transport and grain boundaries behaviors in CdTe were systematically investigated using photon excitation microscopy and scanning probe microscopy.[7–9] The local charge transport in CdTe film is significantly impacted by the grain size, grain boundary passivation, and $CdCl_2$ heat treatment history. Meanwhile, various macroscopic mechanical properties of the bulk and thin film CdTe have also been reported in both experimental and theoretical understanding.[10–12] For example, a significant increase of yield stress was observed in the CdTe crystal while comparing the mechanical measurements performed in the dark and under illumination, suggesting that its mechanical properties are sensitive to light.[10] Also, the mechanical characterization using the nanoindentation technique indicates that the substrate temperature during a deposition could also influence the elastic modulus of the CdTe thin film.[4]

For the flexible electronics applications, CdTe as a soft semiconductor with large lattice mismatch between windows layer CdS may limit the reliability of the flexible CdTe solar cells.[13] In particular, a large amount of dislocation and stack faults in the CdTe film may generate considerable irreversible deformation.[14] However, little experimental investigation is reported on how the nanoscale mechanical reliability in polycrystalline CdTe solar cells impacted by the microstructures. In particular, the nanoscale mechanical behavior of CdTe thin films during solar module working status is lacking, i.e., with the existence of the built-in electric field across the CdTe film, which may contribute to the device degradation besides the well-known ion electromigration induced degradation.[15] The missing knowledge of mechanical degradation makes it difficult to troubleshoot working thin film solar cells reliability issues, create a

target lifespan for the cell, or suggest an enhanced lifetime of solar modules. However, decoupling these mechanical and electrical phenomena can prove to be a challenge. Therefore, the advanced technique of scanning probe microscopy was employed to achieve a high resolution on the intrinsic level of these thin films.[16] It is known that the grain boundary of CdTe plays as the recommendation sites during the carrier transport.[17] In this work, the nanoscale mechanical and electrical properties across the grains and grain boundaries for the as-grown and $CdCl_2$ treated CdTe were systematically investigated to understand the role of grains and grain boundaries in the CdTe solar cells. Meanwhile, the correlation between the electrical field and the localized mechanical response of grain and grain boundary was also characterized to address the potential mechanical deformation induced device degradation. This study could provide an additional view to addressing the thin film solar cells reliability issues within the 25 years warranty.

CdTe thin film solar cells were deposited on sputtered CdS window layer coated F: SnO_2 glass substrate via close-space sublimation, followed by $CdCl_2$ heat treatment.[6,18] The $CdCl_2$ heat treatment was conducted at 430°C for 30 min. Additionally, Copper treatment was performed via a wet process using $CuCl_2$ solution.[19] The solar cell had a superstrate structure as fluorine-doped SnO_2 (FTO)/CdS/CdTe/graphite. Conductive AFM (cAFM) was used to characterize the intrinsic electrical properties of the CdTe thin films with conductive AFM Tips (Cr/Au coated Si Tips). To ascertain the role of grain and grain boundaries in the mechanical performance, a force modulation microscopy (FMM) was used. The correlation between the localized electrical and mechanical response was investigated using a marked area on the CdTe film surface.

Figure 1a shows the XRD spectra indicating the CdTe with zinc blende cubic structure post the $CdCl_2$ treatment, which is a critical process for the CdTe solar cells. Figure 1b shows the SEM image depicting that the chloride activation treatment increases the grain size to 2~3 μm from the grain size of about 1 μm of the as-grown film as shown in the AFM topography image Figure 2a. The devices used for the scanning probe microscopy had a power conversion efficiency ~ 15% represented through the current-voltage (*J-V*) curve shown in Figure 1c. The solar cells current-voltage (J-V) curve was characterized using a solar simulator (Newport, Oriel Class AAA 94063A, 1000 Watt Xenon light source) with a source meter (Keithley 2420) at 100 mW/cm^2 AM 1.5G irradiation. A calibrated Si-reference cell and meter (Newport, 91150V, certificated by National Renewable Energy Lab) was used to calibrate the solar simulator before each measurement. This decent device performance provides us with a good platform to perform the nanoscale characterization of the correlation between localized mechanical and electrical transport behavior. Figure 1d shows the AFM experimental setup for this work, where the FTO substrate was grounded using the silver paste, and the cAFM tips were used for the electrical characterization, and the FMM tips were used to characterize the local mechanical response on the surface of the CdTe films. Both the cAFM and FMM scanning was conducted in the contact mode. Meanwhile, an external electrical field can be applied to the CdTe films to investigate electrical field impacts on the mechanical properties.

Figure 2a and 2d are AFM topography images of as-grown, and $CdCl_2$ treated CdTe thin films, respectively. The grain size was about 1 μm for the as-grown CdTe films, which increased to ~ 3 μm with $CdCl_2$ treatment, which is similar to the SEM image as shown in Fig. 1b. Figure 2b and 2e show the cAFM images for the as-grown and the $CdCl_2$ treated CdTe thin films, respectively. The current images are not limited by the topography images and show nonuniform electrical conductivity. Particularly, the $CdCl_2$ treated CdTe films demonstrates this in several grains. Meanwhile, there is

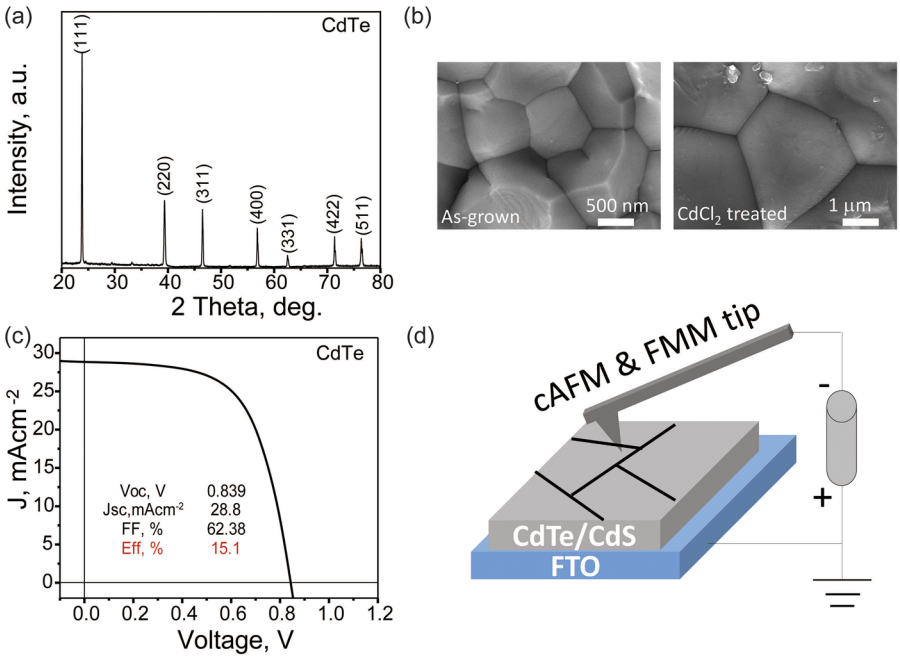

FIG. 1. CdTe devices with 15% power conversion efficiency: (a) X-ray diffraction (XRD) spectrum of the CdTe thin film after $CdCl_2$ treatment. (b) SEM of the CdTe final device, (c) the current density-voltage (*J-V*) curve, and (d) the schematic diagram of the conductive AFM and FMM on CdTe films.

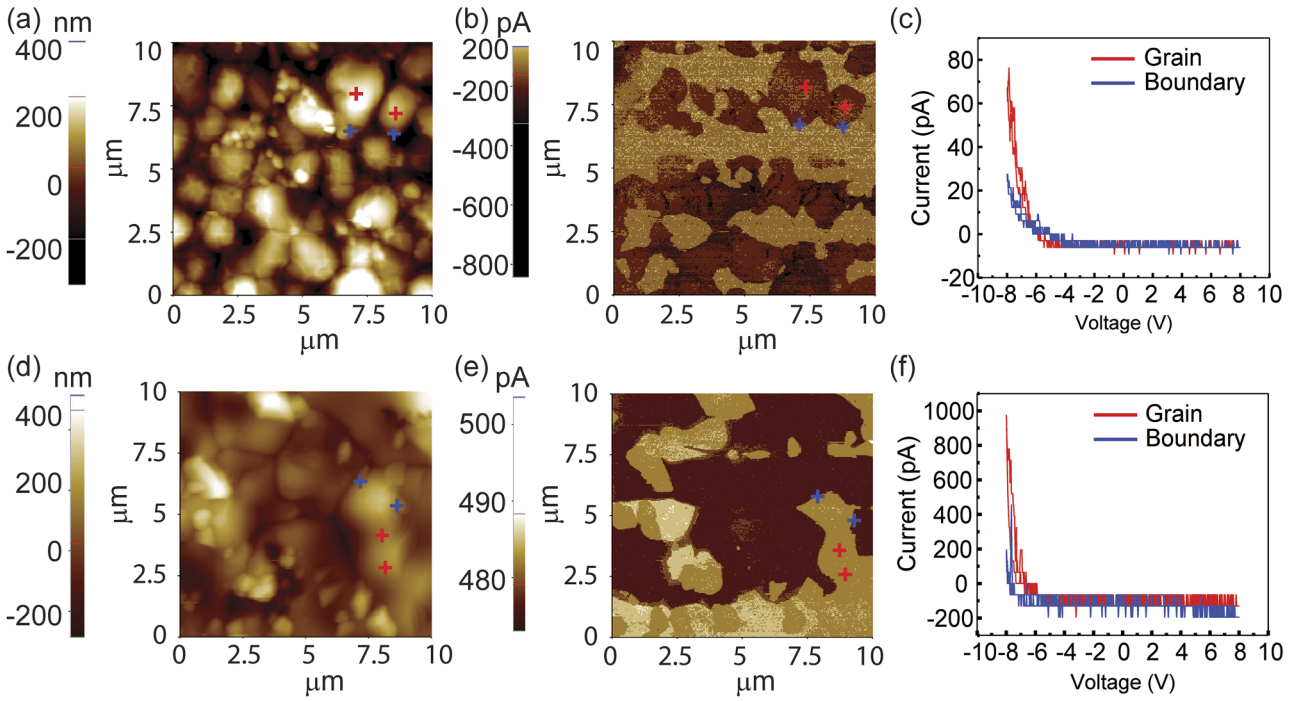

FIG. 2. (a) and (d) AFM topography, (b) and (e) cAFM image, and (c) and (f) localized I-V curve in the grain and boundary for the as-grown and post $CdCl_2$ treated CdTe, respectively. The scan size is 10×10 μm^2.

a conductivity difference between grain boundaries and intragrains for both the as-grown and $CdCl_2$ treated CdTe films. In general, $CdCl_2$ treated CdTe thin films have an increased conductivity, which is in agreement with the previous observation in $CdCl_2$ treated CdTe since the Cl will segregate along the grain boundary and promote the photogenerated carrier transport along the grain boundary.[7] One explanation of this phenomena is that the grain boundaries become more resistive because the Cl^- ions segregate along the grain boundaries and reduce the carrier concentrations at grain boundaries for CdTe.[8,20]

To identify the localized conductivity, the cAFM conductive tip was located at the grain and grain boundaries to form a closed circuit for characterizing local current-voltage (I-V) curve, where the conductive tip acted as the top electrode of the CdTe solar cells. The I-V curves were generated by measuring the current while sweeping the probe bias between -8 to 8 V. The dark current measurements at nanoscale are shown in Fig. 2c and 2f for the as-grown and $CdCl_2$ treated CdTe films, respectively. Each sample has two separate areas scanned for the cAFM images (red for grain and blue for grain boundaries, and repeated at 4 different sites respectively). It was found that the grains show high conductivity than that of the grain boundaries. Additionally, the $CdCl_2$ treatment increased the conductivity of the CdTe film further by one order of magnitude compared to the as-grown CdTe, which could contribute to the improved carrier transport during the working status of a solar cell.[7]

To understand the nanoscale mechanical properties of the CdTe thin films, FMM is performed on the CdTe surface. During the FMM scanning, the film stiffness due to the elastic deformation could be imaged using the AFM tip-tapping on the CdTe surface. The AFM tip collects the topographic image and the elastic properties of the CdTe surface simultaneously using the DC and AC signals applied to the tips, respectively. The amplitude and phase images from the FMM scanning can be directly used to analyze the elastic properties (e.g., stiffness *vs*. softness) of the film. Figure 3a and 3e show the topography of the as-grown and $CdCl_2$ treated CdTe thin films, and the corresponding FMM phase and amplitude images are shown in Fig. 3b, 3f, and Fig. 3c, 3g, respectively. It is observed that the as-grown CdTe film's grain and grain boundaries have varied stiffness properties (e.g., bright grain boundary *vs.* dark grain in Fig. 3b), while the $CdCl_2$ treated CdTe shows more uniform FMM amplitude between grain and grain boundaries as shown in Fig. 3f. The variant stiffness between the as-grown and the $CdCl_2$ treated CdTe film may be attributed to that Cl presents on the grain boundary would fill the dangled bond in the grain boundary, e.g., passivation of the grain boundary.[21,22] Using the AFM force-distance curve, it is possible to quantify the localized stiffness of the grain and grain boundary for these CdTe films. As shown in Fig. 3d and 3h, the grain-interior is harder than the grain boundaries in both specimens, which could be due to the presence of defects in the grain boundary areas for the as-grown CdTe films, or due to excess chemical segregation in the $CdCl_2$ treated CdTe films. Overall, the $CdCl_2$ treated CdTe film is softer than the as-grown film, which can be evident from the differences between AFM cantilever deflection distance and the piezo-extension. The displacement doubled from 0.25 μm to 0.5 μm from the as-grown film to the $CdCl_2$ treated film for the

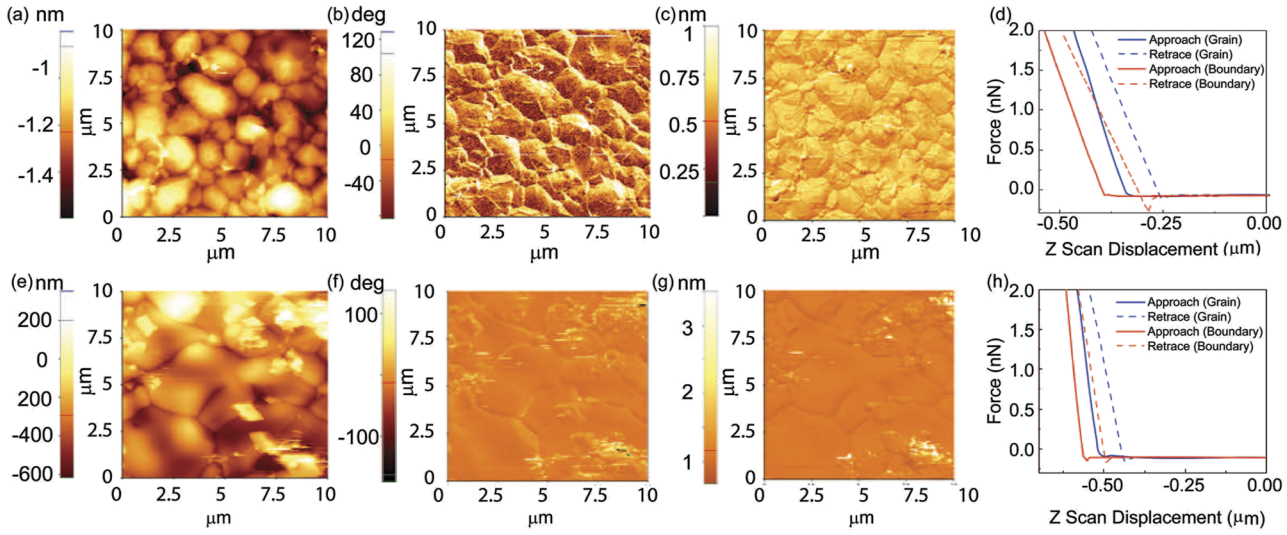

FIG. 3. (a) and (e) The AFM tomography, (b) and (f) force modulation microscopy (FMM) phase image, (c) and (g) amplitude images (10×10 μm^2) and, (d) and (h) localized force-distance curve in the grain and boundary for the as-grown and $CdCl_2$ treated CdTe, respectively.

same applied force (2 nN), confirming that the $CdCl_2$ treatment softens the as-grown CdTe films. In addition, it is found that the grain boundaries in as-grown CdTe film have an adhesion force between the tip and the grain boundaries (as depicted by the red dashed line in Fig. 3d) which is negligible in the CdTe post the $CdCl_2$ treatment (Fig. 3h). This indicates that for the same amount of applied force of 2 nN, the grain boundaries deform more than the grains, and in other words, the grain boundaries can be the initial site for the mechanical deformation failure in the CdTe thin film.

To study the impact of the electric field on the stiffness of the grain and grain boundary in the CdTe film, a 2 V DC bias was applied to the $CdCl_2$ treated CdTe sample. This applied voltage is similar to the current-voltage measurement range of CdTe thin-film solar cells to simulate the working status of the solar cell (from

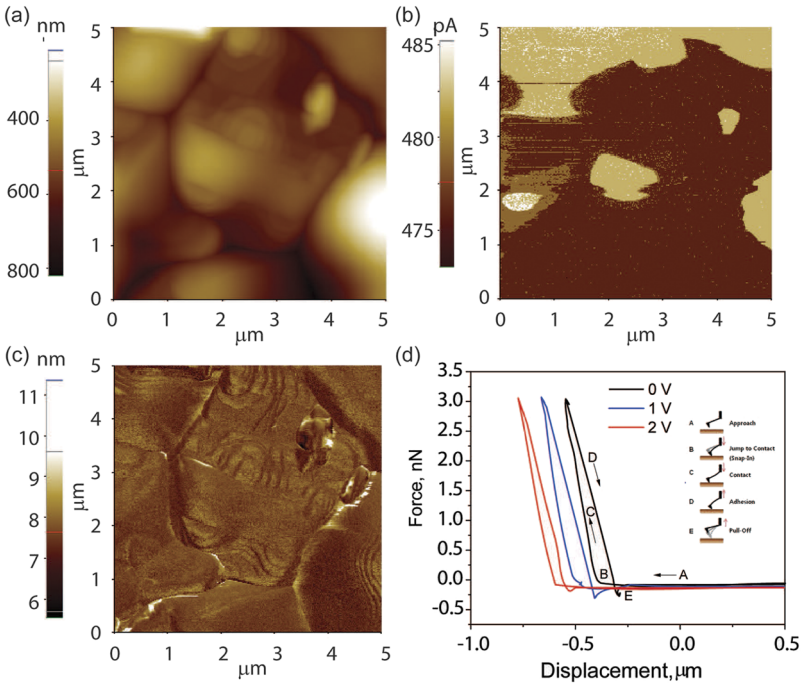

FIG. 4. (a) AFM tomography, (b) the conductive AFM, (c) Force modulus microscopy (FMM) and (d) the force-distance curve under +2 V bias on the $CdCl_2$ treated CdTe films (5×5 μm^2).

-0.5 to 1V). The topography of the film did not change with the applied bias as shown in Fig. 4. However, the cAFM image (Fig. 4b) and the FMM images (Fig. 4c) suggests distinct grain and grain boundary behavior. The grain boundary becomes a larger contrast than that of the intragrain on applying the bias, as shown in Fig. 4c, suggesting that the grain boundary becomes softer than the grain with the existence of the built-in electric field. The potential reason for this electric field induced mechanical deformation is that the ions migration at the grain boundaries is higher than that of the grain, such as the Cl^- or Cu^+ ions during Cl treatment and Cu doping process. Since these ions are easy to form the defect complexes, such as Cl_i-V_{Cd} and Cl_{Te}-V_{Cd} and Cu_{Cd}-Cu_i, the built-in electrical field could break the defect complex at the grain boundaries area and generate more vacancies. Also, the dislocation and twin boundaries could also be moved and pin at the grain boundaries as the molecular dynamics simulated previously, where the interfacial misfit dislocation formed to accommodate the lattice mismatch.[21]

In summary, this study explored the nanoscale electrical and mechanical properties and their correlation in the CdTe thin films solar cells. This work showed that there is a significant difference in the mechanical and electrical properties between the as-grown CdTe and $CdCl_2$ treated CdTe thin films. There is an increased electrical behavior and a decreased elastic stiffness in the $CdCl_2$ treated thin films characterized using the cAFM and FMM. These observations suggest that the $CdCl_2$ treatment could contribute to improved device performance. However, they can also lead to easier mechanical deformation in the CdTe solar cells. By applying a DC bias across the CdTe device, it is observed that the electric field can decrease the stiffness of CdTe thin film. This decrease in stiffness could lead to mechanical deformations in the solar cell and possibly result in mechanical failure along the grain boundary. Thus, any such treatment may need to be addressed during a flexible solar cell application.

Special thanks to Dr. Yanfa Yan and Dr. Corey Grice from the University of Toledo to provide the CdTe samples for these experiments. M. Mathews, L. Guo, F. Yan thank for the support from the University of Alabama startup fund, and NSF award No. 1844210.

REFERENCES

[1] S. G. J. Fritsche, E. Goluda, M. C. Lejard, A. Thiβen, T. Mayer, A. Klein, R. Wendt, R. Gegenwart, D. Bonnet, and W. Jaegermann, Thin Film Solids **387**, 161 (2001).
[2] H. P. Mahabaduge, W. L. Rance, J. M. Burst, M. O. Reese, D. M. Meysing, C. A. Wolden, J. Li, J. D. Beach, T. A. Gessert, W. K. Metzger, S. Garner, and T. M. Barnes, Appl. Phys. Lett. **106**, 133501 (2015).
[3] Z. Bai, J. Yang, and D. Wang, Appl. Phys. Lett. **99**, 143502 (2011).
[4] M. Thangaraju, A. Jayaram, and R. Kandasamy, Appl. Surf. Sci. **449**, 2 (2018).
[5] S. J. Ikhmayies and R. N. Ahmad-Bitar, Physica B **405**, 3141 (2010).
[6] N. R. Paudel and Y. F. Yan, Thin Solid Films **549**, 30 (2013).
[7] J. Luria, Y. Kutes, A. Moore, L. H. Zhang, E. A. Stach, and B. D. Huey, Nat. Energy **1**, 16150 (2016).
[8] C. Li, Y. L. Wu, J. Poplawsky, T. J. Pennycook, N. Paudel, W. J. Yin, S. J. Haigh, M. P. Oxley, A. R. Lupini, M. Al-Jassim, S. J. Pennycook, and Y. F. Yan, Phys. Rev. Lett. **112** (2014).
[9] D. Kuciauskas, D. Lu, S. Grover, G. Xiong, and M. Gloeckler, Appl. Phys. Lett. **111**, 233902 (2017).
[10] G. Purcek, E. Bacaksiz, and I. Miskioglu, J. Mater. Process. Tech. **198**, 202 (2008).
[11] Q. Xiang, X. Peng, H. Yang, H. Xiang, C. Huang, B. Yang, X. Yue, and T. Fu, Ceram. Int. **43**, 14405 (2017).
[12] X. W. Zhou, J. J. Chavez, S. Almeida, and D. Zubia, J. Appl. Phys. **120**, 045304 (2016).
[13] H. Nishino, I. Sugiyama, and Y. Nishijima, J. Appl. Phys. **80**, 3238 (1996).
[14] S.-H. Yoo, K. T. Butler, A. Soon, A. Abbas, J. M. Walls, and A. Walsh, Appl. Phys. Lett. **105**, 062104 (2014).
[15] L. T. Nicholas Strevel, C. Kotarba, and I. Khan, Photovoltaics Int. **22**, 1 (2013).
[16] H. R. Mountinho, R. G. Dhere, C.-S. Jiang, M. M. Al-Jassim, and L. L. Kazmerski, Thin Film Solids **514**, 150 (2006).
[17] H. R. Moutinho, R. G. Dhere, C. S. Jiang, Y. F. Yan, D. S. Albin, and M. M. Al-Jassim, J. Appl Phys. **108**, 074503 (2010).
[18] C. R. Grice, A. Archer, S. Basnet, N. R. Paudel, and Y. Yan, in 43rd IEEE Photovoltaic Specialist Conferences, 2016, p. 1459.
[19] L. Kranz, C. Gretener, J. Perrenoud, R. Schmitt, F. Pianezzi, F. La Mattina, P. Blösch, E. Cheah, A. Chirilă, C. M. Fella, H. Hagendorfer, T. Jäger, S. Nishiwaki, A. R. Uhl, S. Buecheler, and A. N. Tiwari, Nat. Commun. **4**, 2306 (2013).
[20] M. Tuteja, P. Koirala, V. Palekis, S. MacLaren, C. S. Ferekides, R. W. Collins, and A. A. Rockett, J. Phys. Chem. C **120**, 7020 (2016).
[21] J. J. Chavez, X. W. Zhou, S. F. Almeida, R. Aguirre, and D. Zubia, J. Phys. Chem. C **122**, 751 (2018).
[22] C. Li, J. Poplawsky, Y. Yan, and S. J. Pennycook, Mater. Sci. Semicon. Proc. **65**, 64 (2016).